

Published in final edited form as:

*Invest Ophthalmol Vis Sci.* ; 54(13): 8152–8159. doi:10.1167/iovs.13-13230.

## Is Hand-Held Optical Coherence Tomography Reliable in Infants and Young Children with and without Nystagmus?

Helena Lee, MB, FRCOphth<sup>1</sup>, Frank Proudlock, MSc, PhD<sup>\*,1</sup>, and Irene Gottlob, MD, FRCOphth<sup>1</sup>

<sup>1</sup>Ophthalmology Group, University of Leicester, Robert Kilpatrick Clinical Sciences Building, PO Box 65, Leicester Royal Infirmary, Leicester, LE2 7LX

### Abstract

**Purpose**—To evaluate the reliability of the spectral domain hand-held OCT (HH-OCT) in assessing foveal morphology in children with and without nystagmus.

**Methods**—Forty-nine subjects with nystagmus (mean age 43.83 months; range 1-82 months) and 48 controls (mean age 43.02 months; range 0 to 83 months) were recruited and scanned using HH-OCT (Bioptigen). A minimum of 2 separate volumetric scans on the same examination day of the fovea were obtained. The images were imported into ImageJ software where manual retinal layer segmentation of the central foveal B-scan was performed. Agreement between scans was assessed by determining the intraclass correlation coefficients (ICC) and Bland–Altman plots.

**Results**—Both the nystagmus and controls groups showed an excellent degree of reproducibility between two examinations with ICCs greater than 0.96 for central macular thickness (CMT) and greater than 0.8 for the outer nuclear layer and outer segment of the photoreceptors. The nerve fiber layer, ganglion cell layer, outer plexiform layer, inner segment of the photoreceptors and retinal pigment epithelium were less reliable with ICCs of less than 0.7. There was no difference in the reliability of scans obtained in children with nystagmus as compared to controls and both groups had good inter-eye agreement with ICCs greater than 0.94 for CMT.

**Conclusion**—We have shown for the first time that the HH-OCT provides reliable measurements in children with and without nystagmus. This is important as the HH-OCT will have a greater diagnostic and prognostic role in young children with nystagmus and other eye diseases in the future.

### Introduction

Although optical coherence tomography (OCT) has revolutionized diagnosis and treatment in many retinal diseases in adults and older children, infants and children too small to cooperate have been deprived clinically from OCT. A hand-held spectral domain OCT (HH-OCT) which has been optimized for use in infants and young children has demonstrated its

---

**Corresponding author:** Professor Irene Gottlob, Ophthalmology Group, University of Leicester, Robert Kilpatrick Clinical Sciences Building, PO Box 65, Leicester Royal Infirmary, Leicester, LE2 7LX. +441162586291 ; ig15@leicester.ac.uk.

\*Co-first author

**Conflict of Interest:** No conflicting relationship exists for any author

clinical utility in identifying retinal morphology in infants with retinopathy of prematurity (ROP), maculopathy, retinal dystrophy, post traumatic choroidal neovascularization and Leber's congenital amaurosis.<sup>1-8</sup> We have recently shown that the HH-OCT is reliable for diagnosing the etiology of nystagmus.<sup>9</sup>

In older patients with nystagmus, it has been shown that optical coherence tomography (OCT) produces reliable retinal measurements and can differentiate albinism, changes in *PAX6* mutation and achromatopsia from idiopathic nystagmus by identifying typical or atypical foveal hypoplasia.<sup>10-12</sup> It has also been shown that the length of the photoreceptor outer segment is strong predictor of visual acuity in patients with albinism.<sup>11</sup> It has been reported that the images obtained using HH-OCT contain movement artifacts caused by the examiner and/or the child.<sup>8</sup> Also it is unclear if reliable measurements of the retinal layers can be obtained using the HH-OCT in infants and young children with and without nystagmus. In this study we evaluated the reliability of the HH-OCT in assessing foveal morphology in healthy children and children with nystagmus, likely to be one of the most difficult pathologies to image, aged between birth and 6 years of age.

## Patients and Methods

The cohort for this study included 49 children with nystagmus (mean age 43.83 months; standard deviation 24.1 months; range 1-82 months) and 48 control participants (mean age 43.02 months; standard deviation 24.7 months; range 0 to 83 months) in which a minimum of two separate successful OCT scans on at least one eye were obtained on the same day. The demographic data and diagnostic breakdown are summarized in Table 1.

Spectral domain hand-held optical coherence tomography HH-OCT (Bioptigen Envisu system, Durham, NC, USA) was used to obtain a minimum of two separate volumetric scans (consisting of 100 B-scans and 500 A-scans per B-scan) on the same examination day of the foveal region. The acquisition speed for each B scan was 5.8 milliseconds with an overall scan time of 2.9 seconds and a digital resolution of 2.4 microns per pixel. This ensured that any motion artifact caused by nystagmus was minimal. All children were scanned in the outpatient clinic setting without sedation. A total of 166 scans in the nystagmus participants and 164 scans in the healthy controls were obtained. Repeat scans were obtained in at least one eye in all nystagmus subjects (n = 49) and all healthy controls (n = 48). Acquisition of an OCT scan was considered successful if the B scan containing the foveal center was captured together with a minimum of 5 uninterrupted B scans (i.e. without refixations or blinks on either side of the central foveal B scan). The retinal vasculature and optic nerve head were used to determine if refixations had taken place during the scan.

The acquired images were exported from the Bioptigen OCT software and imported into ImageJ software (available at: <http://rsbweb.nih.gov/ij/> Date accessed: May 11, 2012) where retinal layer segmentation was performed by manually identifying each layer at the fovea (Fig 1A and 1B). The fovea was identified by visual inspection of the B scan images for the presence of a foveal depression, thinning of the inner retinal layers, doming of the outer nuclear layer and lengthening of the photoreceptor outer segments as described by Mohammad et al.<sup>11</sup> Measurements of each retinal layer were only performed if the borders

between each adjacent retinal layers were visible. In cases where the border between adjacent retinal layers was not clear a combined measurement of the affected layers was taken (see first section of results).

We analyzed: (1) the reproducibility of retinal layer measurements between separate scans of each participant; (2) the difference in reliability between scans obtained in children with nystagmus as compared to age-matched controls, and (3) the inter-eye agreement on scans obtained from the same subject. Reproducibility between scans was assessed by determining the intraclass correlation coefficient (ICC) and by Bland–Altman assessment. For the test-retest analysis, if repeat scans were present for both eyes only a single eye (the right eye) was analyzed. If two repeated scans were available for only one eye this eye was chosen. A summary of the total number of right and left eyes analyzed is provided in Table 1. If more than two scans were obtained the two highest quality scans were selected for analysis, with the highest quality scan analyzed first so that any bias due to quality of the scan is shown by the test-retest analysis. We determined the quality of each scan based on the clarity of the borders of each retinal layer (Tables 2 and 3). A paired-samples t-test was conducted to determine the effects of age on the reliability of the retinal measurements.

All analyses were considered significant at a type 1 probability value of  $p < 0.05$ . Statistical analysis was performed with SPSS software version 16.0 (SPSS, Inc., Chicago, IL).

The study adhered to the tenets of the Declaration of Helsinki and was approved by the local ethic committee. Informed consent was obtained from all parents/guardians of patients and control subjects participating in this study.

## Results

### Segmentation difficulties

There were several borders between retinal layers that were not easy to identify in a subset of participants. These were:

- i. The external limiting membrane (ELM), i.e. the border between the outer nuclear layer (ONL) and inner segment of the photoreceptors (IS), was difficult to identify clearly in 15 of 48 analyzed eyes in control participants (31.2%). In 24 of 49 analyzed eyes in participants with nystagmus (49%) the ELM was difficult to identify in the foveal area (Table 2 and figures 2C and 2D). Five of the 49 participants with nystagmus were achromats in whom the IS was disrupted by a hypo reflective zone and therefore could not be analyzed. The ELM appeared more difficult to identify in the younger participants in both groups. The mean age at which the ELM was clearly identified was 53.25 months and 45.61 months in the nystagmus and control groups respectively. In comparison to this, the mean age of the participants where the ELM was not visible was 23.17 months and 18.67 months in the nystagmus and control groups respectively. However the effect of age was not significant in either the control participants ( $p = 0.596$ ) or the nystagmus participants ( $p = 0.093$ ).

- ii. The border between the outer segment of the photoreceptors (OS) and the retinal pigment epithelium (RPE) although present on all scans was often indistinct preventing accurate demarcation (for example see magnified region of figure 2D). Consequently it was difficult to identify the border in 9 of 48 analyzed eyes in control participants (18.8%) and in 13 of 49 analyzed eyes in participants with nystagmus (26.5%) (Table 3). The mean age at which this border was clearly identified was 44.75 months and 49.26 months in the nystagmus and control groups respectively. In comparison to this, the mean age of the participants where this border was not clear was 38.23 months and 20.33 months in the nystagmus and control groups respectively. This border was significantly more difficult to delineate in the younger participants of the control group ( $p = 0.029$ ). The effect of age did not reach significance in the nystagmus group ( $p = 0.097$ ).
- iii. In the case of foveal hypoplasia, in the nystagmus group, the border between the ganglion cell layer (GCL) and inner plexiform layer (IPL) could be difficult to identify. The border was not clearly visible in 14 of the 28 participants (50%) with foveal hypoplasia, where these layers were present (Table 3) (Fig 2C and 2D). There was no significant age difference between any of the segmentation categories of this group ( $p = 0.574$ ). This border could be visualized clearly in 43.2% and 50% of the albinism and *PAX6* participants respectively. This was most difficult to identify in achromatopsia, with the border being clearly identified in only 25% of the achromatopsia participants.

We have provided measurements of the combined layers: IS-ONL; OS-RPE and GCL-IPL in tables 2 and 3 in order to take the difficulties with accurate segmentation of these borders into account.

### Reproducibility of retinal measurements between scans

Both the nystagmus and controls groups demonstrated excellent reproducibility between two examinations for central macular thickness (CMT) with ICCs greater than 0.96.

In general measurement of the outer retinal layers showed a good degree of reproducibility with ICCs of between 0.8 and 0.95 for the ONL, OS, combined ONL-IS and combined OS-RPE measurements in both the nystagmus and control groups. The test-retest reliability of the IS and RPE measurements were not as consistent with ICCs of 0.626 and 0.671, respectively in the nystagmus group. The ICCs were 0.557 and 0.305, respectively in the control group.

For the inner retinal layers which were present in the fovea in patients with foveal hypoplasia in the nystagmus group there was a good degree of reproducibility for the IPL, INL and combined GCL-IPL measurements with ICCs of 0.741, 0.778 and 0.870, respectively. The test-retest reliability of the other inner retinal layers; the nerve fiber layer (NFL); GCL and outer plexiform layer (OPL) was not as consistent with ICCs of 0.481, 0.623 and 0.401, respectively. The ICCs were comparable between both groups showing that there is no difference in the reliability of scans obtained in children with nystagmus as compared to age-matched healthy controls (Tables 2 and 3).

**Inter-eye comparison of nystagmus and control subjects**—Scans of both eyes were compared in 47 of the nystagmus subjects and 45 of the control subjects. Both the nystagmus and controls groups showed a good degree of inter-eye agreement with ICCs greater than 0.94 for CMT (Tables 2 and 3 and Fig 1C).

### Bland-Altman assessment

A Bland-Altman assessment for agreement was used to compare the two separate measurements (Table 4). With the exception of the CMT and combined OS-RPE measurements in the control group and the INL, OPL and combined OS-RPE measurements in the nystagmus group, bias was not significantly different from zero in both groups for all retinal layer measurements.

There was a significant positive bias in the CMT and combined OS-RPE measurements in the control group with a biases of 0.291 ( $p = 0.044$ ) and 0.484 ( $p < 0.0001$ ) respectively, indicating a trend towards larger thickness measurements for these layers with better quality scans. There was also a significant positive bias in the OS and combined OS-RPE measurement in the nystagmus group with a bias of 0.402 ( $p = 0.008$ ) and 0.647 ( $p < 0.0001$ ) respectively, indicating a trend towards a larger thickness measurement for this layer with higher quality scans.

There was a significant negative bias in the measurements if the INL and OPL in the nystagmus group with biases of  $-0.615$  ( $p < 0.000$ ) and  $-0.609$  ( $p = 0.001$ ) respectively, indicating a trend towards smaller thickness measurements for these layers with higher quality scans.

The 95% limits of agreement that were established ranged from a minimum interval of  $-1.0$  to  $2.8$  for the OS; a maximum interval of  $-3.2$  to  $3.4$  for the ONL in the control group; a minimum interval of  $-1.7$  to  $2.2$  for the RPE and a maximum interval of  $-6.7$  to  $5.4$  for the combined ONL and IS measurement in the nystagmus group. The limits of agreement were narrower in control as compared to the patient group. The limits of agreement between patients and controls are of similar ranges and small enough for clinical tests.

### Discussion

We have demonstrated for the first time that the HH-OCT produces reliable assessments of foveal morphology in young children with and without nystagmus. The ICCs for CMT were excellent with an ICC of 0.966 in the nystagmus group and 0.960 in the control group. These are only marginally lower those obtained in adult patients with nystagmus (0.97) and adult controls (0.98).<sup>12</sup> This should be expected as the inner limiting membrane (ILM) and Bruch's membrane exhibit the strongest signals on OCT. The ICCs for ONL and OS were also high with ICCs  $>0.8$  in the nystagmus and in the control group respectively. Reliable quantification of the OS is important clinically as this can potentially be used as an objective predictor of visual acuity.<sup>11</sup> Bland-Altman plots showed good agreement for both groups for intraretinal thickness measurements and the 95% limits of agreement were comparable to those reported in adults with and without nystagmus.<sup>12</sup>

We have also identified which retinal layers may be less reliable when quantified. This includes the GCL and OPL layers in the nystagmus group and the IS and RPE layers in both the nystagmus and control groups. The GCL and OPL layers have very similar reflectance profiles making their borders more difficult to delineate accurately. This leads to a poor signal-to-noise ratio when image quality is not be of sufficient standard to allow accurate quantification of these layers.

Comparing the consistency of measurements based on whether the borders between individual layers are clear or not clear did improve the ICCs for the IS from 0.289 to 0.626 in the nystagmus group and from 0.367 to 0.557 in the control group. However the ICCs did not reach the same level of reliability as the other retinal layers such as ONL. Also comparing the consistency of measurements based on border clarity did not improve the ICCs for the OPL in the nystagmus group and the RPE in both the nystagmus and control groups. As these layers are much thinner than the other layers of the fovea their measurements are likely to be more sensitive to errors such as measurement error and quantization effects. The ICCs obtained in this study were higher with the thicker retinal layers making this a plausible explanation.

One other explanation that would need to be considered is that in infants and young children the retinal layers are developing. Histological studies of the simian<sup>13-15</sup> and human<sup>16, 17</sup> retina have demonstrated that macular development is a sophisticated process which involves the outward displacement of the inner retinal layers (GCL, INL and IPL) and inward migration of the cone photoreceptors into the fovea. This process is thought not be complete until between 11 months of age and 5 years.<sup>16-19</sup> Over time, the cone photoreceptors become taller, narrower and more tightly packed as the fovea matures. It has been reported that the space between the ELM (which represents the ellipsoid of the inner segment of the photoreceptors<sup>20</sup>) and the RPE measures only 14  $\mu\text{m}$  at the fovea at birth.<sup>17</sup> At 13 months of age the length of the foveal IS/OS are 36  $\mu\text{m}$ .<sup>17</sup> By 13 years of age the photoreceptors have reached adult values, with the foveal IS measuring between 168  $\mu\text{m}$  and 189  $\mu\text{m}$  and the OS measuring between 139  $\mu\text{m}$  and 155  $\mu\text{m}$  long.<sup>17</sup>

It is possible that in the immature retina, structures such as the ELM, may not be visible on OCT until they have matured sufficiently. We observed a tendency towards more difficulties with segmentation of the ELM and the junction between the OS and RPE in the younger participants of both groups. This did not reach statistical significance for the ELM in both groups and for the junction between the OS and RPE in the nystagmus group. The effect of age did reach significance, however, for the junction between the OS and RPE in the control group ( $p = 0.029$ ).

We attempted to improve the reliability of measurements of these retinal layers, by performing combined measurements of the retinal layers where it was apparent that there were difficulties with delineating their borders. This affected the GCL-IPL layers; the ONL-IS layers and the OS-RPE layers. Assessment of these combined layers was consistent on test-retest analysis with ICCs of 0.870, 0.931 and 0.933, respectively, for the nystagmus group. The ICCs were 0.931 and 0.870 for the combined ONL-IS layer and combined OS-RPE layers, respectively, in the control group. This is a strategy that potentially could be



used to improve reliability when using HH-OCT to quantify normal retinal development, identify retinal pathology and in developing objective OCT based predictors of visual acuity.

Another factor to consider is that the subjective nature of the manual segmentation of the inner retinal layers may have contributed to the reduction in the reproducibility of the measurements of the inner retinal layers. The development of automated retinal layer segmentation and quantification software may help to further improve the reliability of the HH-OCT by removing this factor.

There was a trend towards a larger estimate of CMT measurements in the control group; OS measurement in the nystagmus group and combined OS and RPE measurements in both the nystagmus and control groups with higher quality images. This may be accounted for by the increased reflectance of the RPE border and IS/OS junction in the higher quality images, which make the RPE and OS appear thicker. The trend towards a larger estimate of measurement of the INL and OPL on lesser quality images may be explained by low reflectivity of the borders of these layers leading to an overestimation of thickness of these layers as their borders are not clearly delineated. The effects of image quality on the reliability of these measurements need to be taken into account if the HH-OCT is potentially going to be used in a clinically diagnostic and monitoring role in children with retinal conditions.

It has been previously shown that human foveal development as visualized by spectral-domain OCT correlates anatomically with histologic specimens.<sup>21, 22</sup> Accurate assessment of foveal morphology is important as the HH-OCT will likely play an increasingly important diagnostic and prognostic role in infants and young children with nystagmus and other eye diseases such as ROP and glaucoma. Reliability between measurements will allow accurate monitoring of both normal and abnormal foveal development.

A limitation of this study is that our analysis was limited to the central foveal B-scan. The Bioptigen HH-OCT does not provide automatic motion stabilization to compensate for eye and head movements or movement of the probe when sampling. Consequently, the ability to successfully acquire a volumetric data sequence is much lower compared to adults. In addition, it has been shown that image inversion using spectral-domain OCT optimizes both the choroidal detail visualized and the choroidal thickness measurements obtained.<sup>23</sup> In the future, it would be interesting to also evaluate the test-retest reliability of this image inversion technique using the Bioptigen HH-OCT.

In this study we have shown that the reliability of quantitative central macular thickness and photoreceptor outer segment length measurements using the HH-OCT in children are excellent and is comparable to adult OCT.<sup>12</sup> An OCT-based structural grading system for foveal hypoplasia has been developed previously showing that the grade of arrested foveal development is correlated to VA in a range of disorders associated with foveal hypoplasia.<sup>24</sup> The reliability of the measurement of the length of the photoreceptor outer segment is important as this is a strong predictor of visual acuity in albinism<sup>11</sup> and potentially could help predict visual acuity in various other diseases. Our results provide an important basis for future use of OCT in infants and young children for research and clinical application. In

future studies it would be important, for example, to analyze whether foveal morphology on OCT scans could be used to possibly predict visual acuity in preverbal children, especially as OS have been shown very reliable. Our results support that OCT can be used reliably clinically in young children, in diseases including foveal hypoplasia or can be used to monitor retinal dystrophies especially in view of imminent genetic therapy.

## Acknowledgments

**Financial support:** Medical Research Council, London, UK (grant number: MR/J004189/1), Ulverscroft Foundation, Leicester, UK and Nystagmus Network UK.

## References

1. Scott AW, Farsiu S, Enyedi LB, et al. Imaging the infant retina with a hand-held spectral-domain optical coherence tomography device. *Am J Ophthalmol*. 2009; 147:364–73 e2. [PubMed: 18848317]
2. Maldonado RS, Izatt JA, Sarin N, et al. Optimizing hand-held spectral domain optical coherence tomography imaging for neonates, infants, and children. *Invest Ophthalmol Vis Sci*. 2010; 51:2678–85. [PubMed: 20071674]
3. Maldonado RS, O'Connell RV, Sarin N, et al. Dynamics of human foveal development after premature birth. *Ophthalmology*. 2011; 118:2315–25. [PubMed: 21940051]
4. Maldonado RS, O'Connell R, Ascher SB, et al. Spectral-domain optical coherence tomographic assessment of severity of cystoid macular edema in retinopathy of prematurity. *Arch Ophthalmol*. 2012; 130:569–78. [PubMed: 22232366]
5. Lee AC, Maldonado RS, Sarin N, et al. Macular features from spectral-domain optical coherence tomography as an adjunct to indirect ophthalmoscopy in retinopathy of prematurity. *Retina*. 2011; 31:1470–82. [PubMed: 21792089]
6. Vinekar A, Avadhani K, Sivakumar M, et al. Understanding clinically undetected macular changes in early retinopathy of prematurity on spectral domain optical coherence tomography. *Invest Ophthalmol Vis Sci*. 2011; 52:5183–8. [PubMed: 21551410]
7. Chavala SH, Farsiu S, Maldonado R, et al. Insights into advanced retinopathy of prematurity using handheld spectral domain optical coherence tomography imaging. *Ophthalmology*. 2009; 116:2448–56. [PubMed: 19766317]
8. Gerth C, Zawadzki RJ, Heon E, et al. High-resolution retinal imaging in young children using a handheld scanner and Fourier-domain optical coherence tomography. *J Aapos*. 2009; 13:72–4. [PubMed: 19121595]
9. Lee HSV, Bibi M, et al. Potential of Hand-Held Optical Coherence Tomography to Determine Etiology of Infantile Nystagmus in Children based on Foveal Morphology. *Ophthalmology*. 2013; 120:2714–2724. [PubMed: 24161406]
10. Thomas MG, Kumar A, Kohl S, et al. High-resolution in vivo imaging in achromatopsia. *Ophthalmology*. 2011; 118:882–7. [PubMed: 21211844]
11. Mohammad S, Gottlob I, Kumar A, et al. The functional significance of foveal abnormalities in albinism measured using spectral-domain optical coherence tomography. *Ophthalmology*. 2011; 118:1645–52. [PubMed: 21570122]
12. Thomas MG, Kumar A, Thompson JR, et al. Is high-resolution spectral domain optical coherence tomography reliable in nystagmus? *Br J Ophthalmol*. 2011
13. Dorn EM, Hendrickson L, Hendrickson AE. The appearance of rod opsin during monkey retinal development. *Invest Ophthalmol Vis Sci*. 1995; 36:2634–51. [PubMed: 7499086]
14. Hendrickson A, Kupfer C. The histogenesis of the fovea in the macaque monkey. *Invest Ophthalmol Vis Sci*. 1976; 15:746–56. [PubMed: 822712]
15. Hendrickson A. A morphological comparison of foveal development in man and monkey. *Eye*. 1992; 6(Pt 2):136–44. [PubMed: 1624035]



16. Hendrickson AE, Yuodelis C. The morphological development of the human fovea. *Ophthalmology*. 1984; 91:603–12. [PubMed: 6462623]
17. Yuodelis C, Hendrickson A. A qualitative and quantitative analysis of the human fovea during development. *Vision Res*. 1986; 26:847–55. [PubMed: 3750868]
18. Abramov I, Gordon J, Hendrickson A, et al. The retina of the newborn human infant. *Science*. 1982; 217:265–7. [PubMed: 6178160]
19. Dubis AM, Costakos DM, Subramaniam CD, et al. Evaluation of normal human foveal development using optical coherence tomography and histologic examination. *Arch Ophthalmol*. 2012; 130:1291–300. [PubMed: 23044942]
20. Spaide RF, Curcio CA. Anatomical correlates to the bands seen in the outer retina by optical coherence tomography: literature review and model. *Retina*. 2011; 31:1609–19. [PubMed: 21844839]
21. Hendrickson A, Possin D, Vajzovic L, et al. Histologic Development of the Human Fovea From Midgestation to Maturity. *Am J Ophthalmol*. 2012; 154:767–778. [PubMed: 22935600]
22. Vajzovic L, Hendrickson AE, O'Connell RV, et al. Maturation of the Human Fovea: Correlation of Spectral-Domain Optical Coherence Tomography Findings With Histology. *Am J Ophthalmol*. 2012
23. Lin P, Mettu PS, Pomerleau DL, et al. Image inversion spectral-domain optical coherence tomography optimizes choroidal thickness and detail through improved contrast. *Invest Ophthalmol Vis Sci*. 2012; 53:1874–82. [PubMed: 22410550]
24. Thomas MG, Kumar A, Mohammad S, et al. Structural grading of foveal hypoplasia using spectral-domain optical coherence tomography a predictor of visual acuity? *Ophthalmology*. 2011; 118:1653–60. [PubMed: 21529956]

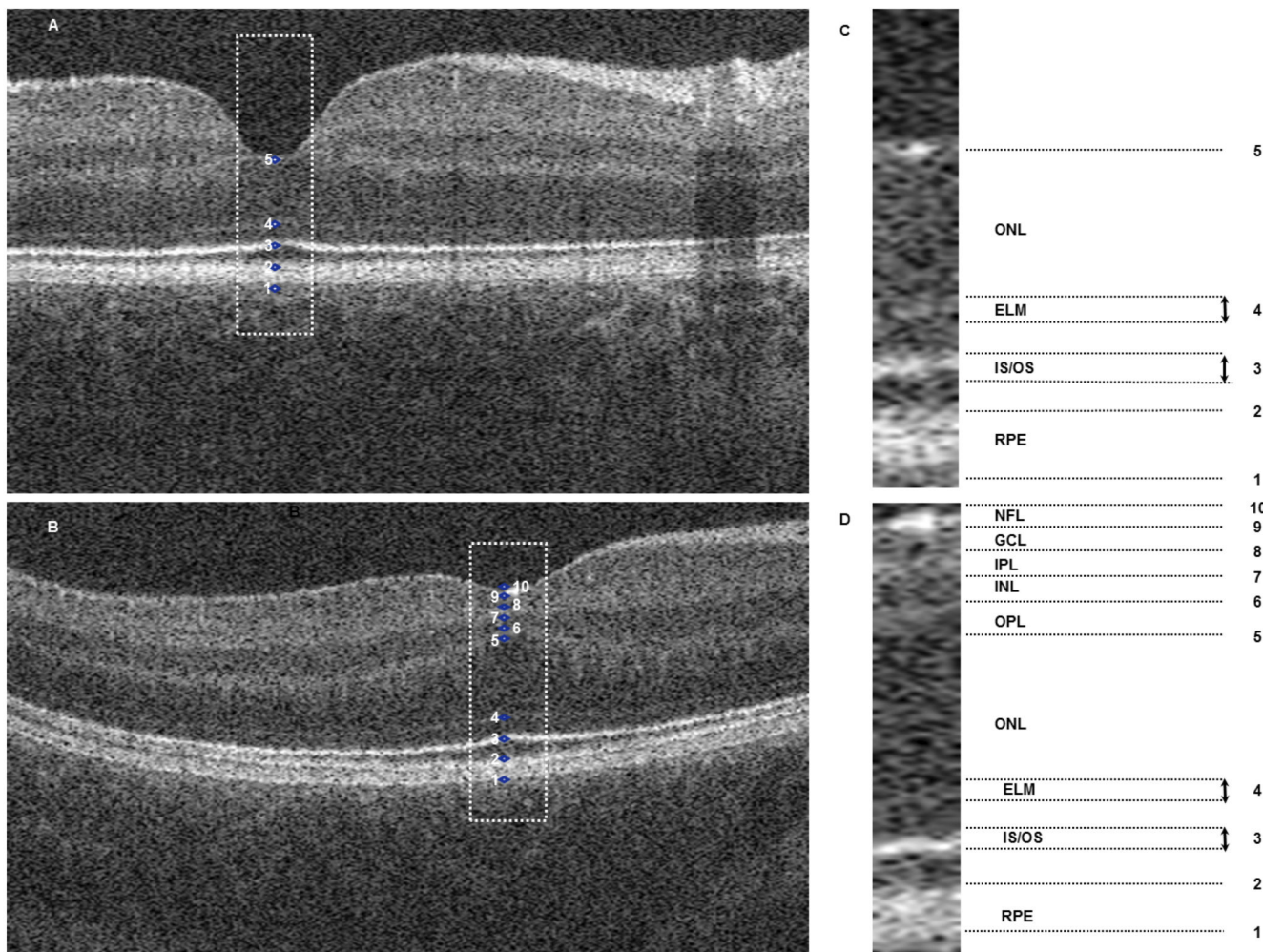


**Figure 1. Optical coherence tomograms of 1 control subjects (1A) and 1 nystagmus subjects (1B).** Segmentation of the foveal B scans was performed using ImageJ software which identified ten points (1C and 1D). These points represented: 1 to 2= RPE; 2 to 3= OS; 3= IS/OS junction; 3 to 4= IS; 4 ELM; 4 to 5= ONL, 5 to 6= OPL; 6 to 7= INL; 7 to 8= IPL; 8 to 9=GCL; 9 to 10= NFL. NFL= nerve fiber layer; GCL= ganglion cell layer; IPL= inner plexiform layer; INL= inner nuclear layer; OPL= outer plexiform layer; ONL= outer nuclear layer; ELM= external limiting membrane; IS/OS= inner segment/outer segment junction; RPE= retinal pigment epithelium.

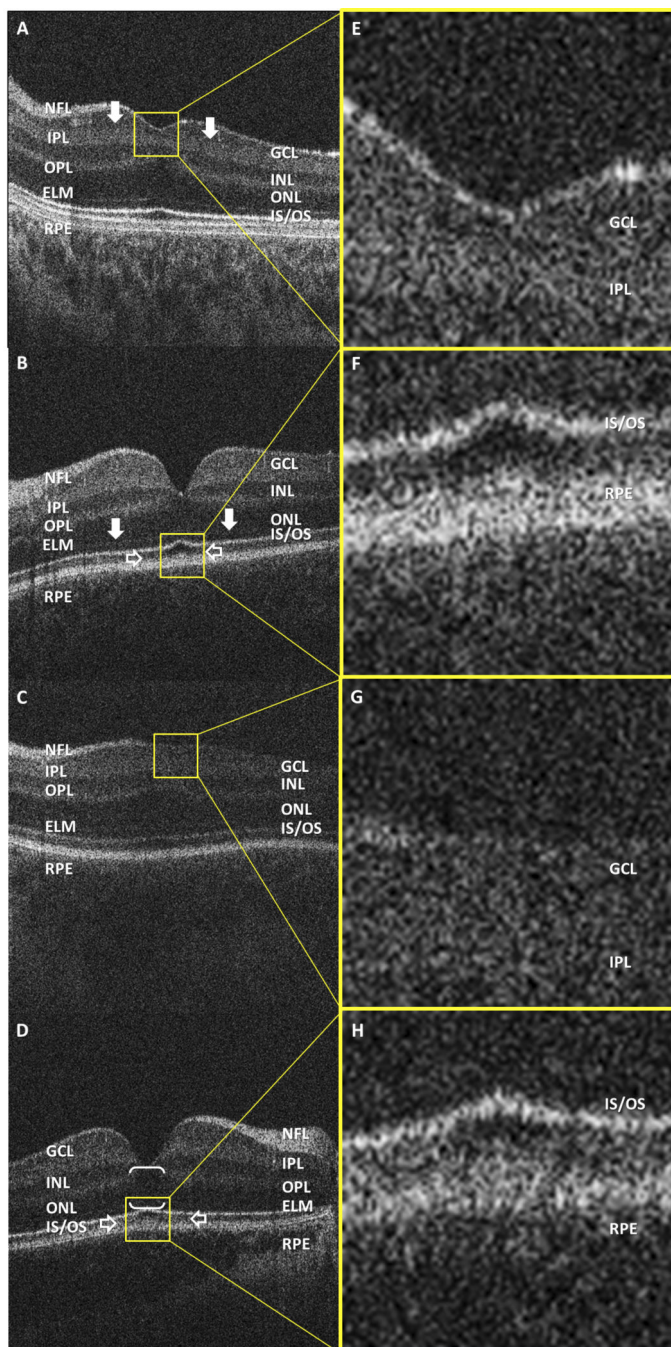


**Figure 2. Optical coherence tomograms of 2 nystagmus subjects (2A and 2C) and 2 control subjects (2B and 2D).**

Examples of the difficulties encountered in the segmentation of the retinal layers are shown. The border between the GCL and IPL (indicated by the arrows in Fig 2A) is often difficult to identify. If the border between these layers could not be delineated, then a combined measurement was taken from the GCL and IPL. A magnified section of the GCL and IPL in Fig 2B and 2D which is indicated by the yellow box is shown in Figs 2A and 2C. The ELM (indicated by the arrows in Fig 2B) is often difficult to delineate (Fig 2D). If the ELM could not be identified then a combined measurement was taken from the ONL and IS. The upper

border of the RPE can be non-distinct (indicated by the open arrows in Fig 2D). If this occurred then a combined measurement was taken from the OS and RPE. A magnified section of the border between the OS and RPE as indicated by the yellow box in Fig 2B and 2D is shown in Fig 2F and 2H respectively.

NFL= nerve fiber layer; GCL= ganglion cell layer; IPL= inner plexiform layer; INL= inner nuclear layer; OPL= outer plexiform layer; ONL= outer nuclear layer; ELM= external limiting membrane; IS/OS= inner segment/outer segment junction; RPE= retinal pigment epithelium; ICC=intraclass correlation coefficient.

**Table 1**  
**Summary of demographic data and diagnostic category of participants**

Category	Age Range (months)	Mean Age (months) (SD)	Gender		Eye Analyzed	
			Male	Female	Right	Left
<b>Control n = 48</b>	0 to 83	43.83 (24.69)	n = 25	n = 23	n = 33	n = 15
<b>Albinism n = 27</b>	1 to 82	41.81 (22.93)	n = 17	n = 10	n = 20	n = 7
<b>IIN n = 11</b>	7 to 81	43.82 (28.06)	n = 10	n = 1	n = 6	n = 5
<b>Achromatopsia n = 4</b>	2 to 70	27.25 (30.02)	n = 2	n = 2	n = 1	n = 3
<b>Patients with <i>PAX6</i> mutations n = 3</b>	48 to 76	59.67 (14.57)	n = 2	n = 1	n = 2	n = 1
<b>Retinal Dystrophy n = 3</b>	45 to 77	57.67 (17.01)	n = 2	n = 1	n = 3	-----
<b>Latent Nystagmus n = 1</b>	-----	36	n = 1	-----	n = 1	-----

n = sample size; IIN = idiopathic infantile nystagmus; SD = standard deviation



Table 2

**Reproducibility of first to second scan measurements of each outer retinal layer.**

The data from one eye of each subject was classified into one of four categories based on border clarity. If there was a difference in the classification of the first and second scan data sets from the same eye, then that eye was placed in the lower quality category. The ICCs were only calculated where  $n > 5$ . The inter-eye correlation is also shown for each retinal layer for both groups.

Retinal layer	Control (n=48 for ICC of repeated measures from one eye) (n=45 for ICC of inter-eye comparison)						Nyctagmus (n=49 for ICC of repeated measures from one eye) (n=47 for ICC of inter-eye comparison)									
	Clear		Not Clear		Not Visible		Not Present		Clear		Not Clear		Not Visible		Not Present	
	ICC (n)	Inter-Eye (n)	ICC (n)	Inter-Eye (n)	ICC (n)	Inter-Eye (n)	ICC (n)	Inter-Eye (n)	ICC (n)	Inter-Eye (n)	ICC (n)	Inter-Eye (n)	ICC (n)	Inter-Eye (n)	ICC (n)	Inter-Eye (n)
<b>CMT</b>	0.960 n = 47	0.947 n = 44	n = 1	n = 1	n = 0	n = 0	n = 0	n = 0	0.966 n = 42	0.987 n = 40	0.982 n = 6	0.341 n = 7	n = 1	n = 0	n = 0	n = 0
<b>ONL</b>	0.887 n = 31	0.820 n = 19	0.928 n = 16	0.808 n = 24	n = 1	n = 1	n = 0	n = 1	0.932 n = 22	0.877 n = 12	0.858 n = 25	873 n = 32	n = 2	n = 3	n = 0	n = 0
<b>IS</b>	0.557 n = 33	0.517 n = 25	0.367 n = 12	0.704 n = 17	n = 3	n = 3	n = 0	n = 0	0.626 n = 20	0.583 n = 12	0.289 n = 18	0.699 n = 22	n = 6	n = 8	n = 5	n = 5
<b>ONL and IS</b>	0.931 n = 46	0.897 n = 44	n = 2	n = 1	n = 0	n = 0	n = 0	n = 0	0.931 n = 35	0.878 n = 29	0.633 n = 9	0.911 n = 13	n = 2	n = 2	n = 3	n = 3
<b>OS</b>	0.872 n = 38	0.695 n = 36	0.343 n = 8	0.426 n = 8	n = 0	n = 0	n = 2	n = 1	0.828 n = 33	0.742 n = 26	0.588 n = 9	0.816 n = 12	n = 1	n = 33	n = 6	n = 6
<b>RPE</b>	0.305 n = 39	0.501 n = 36	0.822 n = 9	0.7 n = 9	n = 0	n = 0	n = 0	n = 0	0.671 n = 36	0.624 n = 29	0.687 n = 13	0.560 n = 18	n = 0	n = 0	n = 0	n = 0
<b>OS and RPE</b>	0.870 n = 48	0.914 n = 45	n = 0	n = 0	n = 0	n = 0	n = 0	n = 0	0.933 n = 49	0.943 n = 47	n = 0	n = 0	n = 0	n = 0	n = 0	n = 0

Clear = Borders of the retinal layer can be delineated accurately

Not Clear = Borders of the retinal layer are visible but indistinct making delineation inaccurate

Not Visible = Retinal layer is visible but the delineating borders are not visible

Not Present = Retinal layer is not present

ICC = intraclass correlation coefficient; n = sample size; CMT = central macular thickness; ONL = outer nuclear layer; ELM = external limiting membrane; IS = inner segment of photoreceptor; OS = outer segment of photoreceptor; RPE = retinal pigment epithelium



**Table 3**  
**Reproducibility of first to second scan measurements of each inner retinal layer.**

The data from one eye of each subject was classified into one of four categories based on border clarity. If there was a difference in the classification of the first and second scan data sets from the same eye, then that eye was placed in the lower quality category. The ICCs were only calculated where  $n > 5$ . The inter-eye correlation is also shown for each retinal layer for both groups.

Retinal layer	Nystagmus (n=49 for ICC of repeated measures from one eye) (n=47 for ICC of inter-eye comparison)							
	Clear		Not Clear		Not Visible		Not Present	
	ICC (n)	Inter-Eye (n)	ICC (n)	Inter-Eye (n)	ICC (n)	Inter-Eye (n)	ICC (n)	Inter-Eye (n)
<b>NFL</b>	0.481 n = 24	0.721 n = 20	n = 2	0.369 n = 5	n = 1	n = 1	n = 22	n = 21
<b>GCL</b>	0.623 n = 14	0.750 n = 9	-0.313 n = 12	0.581 n = 14	n = 2	n = 3	n = 21	n = 21
<b>IPL</b>	0.741 n = 16	0.781 n = 10	0.425 n = 13	0.218 n = 15	n = 4	n = 6	n = 16	n = 16
<b>GCL and IPL</b>	0.870 n = 24	0.819 n = 19	n = 4	0.833 n = 6	n = 3	n = 4	n = 18	n = 18
<b>INL</b>	0.778 n = 23	0.760 n = 18	0.602 n = 5	0.684 n = 6	n = 5	n = 7	n = 16	n = 16
<b>OPL</b>	0.401 n = 21	0.536 n = 13	0.845 n = 7	0.597 n = 10	n = 5	n = 8	n = 16	n = 16

Clear = Borders of the retinal layer can be delineated accurately

Not Clear = Borders of the retinal layer are visible but indistinct making delineation inaccurate

Not Visible = Retinal layer is visible but the delineating borders are not visible

Not Present = Retinal layer is not present

ICC = intraclass correlation coefficient; n = sample size; CMT = central macular thickness; NFL= nerve fiber layer; GCL= ganglion cell layer; IPL= inner plexiform layer; INL= inner nuclear layer; OPL= outer plexiform layer

**Table 4**  
**Summary of Bland-Altman plot for measurements of each retinal layer.**

The higher quality scan was always analyzed first so that any bias due to image quality could be detected.

Control n = 48				Nystagmus n = 49			
Retinal Layer	Mean ( $\mu$ m) (SD)	95% Limits of agreement	Bias (p Value)	Retinal Layer	Mean ( $\mu$ m) (SD)	95% Limits of agreement	Bias (p Value)
<b>CMT n = 48</b>	192.100 (24.957)	-3.8 to 2.3	0.291* (0.044)	CMT n = 48	240.908 (61.075)	-7.5 to 4.1	-0.066 (0.656)
<b>NFL n = 1</b>	-----	-----	-----	NFL n = 26	9.479 (3.962)	-4.9 to 0.2	0.058 (0.777)
<b>GCL n = 1</b>	-----	-----	-----	GCL n = 26	25.864 (8.288)	-4.3 to 6.4	0.092 (0.653)
<b>IPL n = 4</b>	-----	-----	-----	IPL n = 29	30.552 (9.455)	-4.6 to 4.2	0.139 (0.472)
<b>GCL and IPL n = 1</b>	-----	-----	-----	GCL and IPL n = 28	53.959 (20.355)	-6.4 to 4.4	0.290 (0.134)
<b>INL n = 4</b>	-----	-----	-----	INL n = 28	53.959 (20.355)	-6.2 to 4.4	-0.615* (0.000)
<b>OPL n = 4</b>	-----	-----	-----	OPL n = 28	18.893 (8.069)	-5.3 to 1.4	-0.609* (0.001)
<b>ONL n = 47</b>	96.049 (18.004)	-3.2 to 3.4	0.139 (0.350)	ONL n = 47	90.332 (22.557)	-5.2 to 3.8	0.080 (0.592)
<b>IS n = 45</b>	29.340 (5.234)	-3.5 to 0.8	-0.700 (0.648)	IS n = 38	26.871 (4.503)	-0.2 to 4.0	-0.830 (0.620)
<b>ONL and IS n = 45</b>	125.811 (20.261)	-3.9 to 2.6	0.196 (0.197)	ONL and IS n = 42	118.081 (22.498)	-6.7 to 5.4	0.060 (0.704)
<b>OS n = 46</b>	37.409 (8.031)	-1.0 to 2.8	0.089 (0.556)	OS n = 42	32.607 (7.664)	-1.3 to 3.5	0.402* (0.008)
<b>RPE n = 48</b>	27.325 (5.091)	-0.9 to 2.9	0.210 (0.152)	RPE n = 49	25.753 (5.807)	-1.7 to 2.2	-0.117 (0.424)
<b>OS and RPE n = 48</b>	62.575 (13.377)	-2.5 to 3.1	0.484* (0.000)	OS and RPE n = 49	53.898 16.927	-2.9 to 2.1	0.647* (0.000)

n = sample size; CI = confidence interval; CMT = central macular thickness; NFL= nerve fiber layer; GCL= ganglion cell layer; IPL= inner plexiform layer; INL= inner nuclear layer; OPL= outer plexiform layer; ONL= outer nuclear layer; ELM= external limiting membrane; IS = inner segment of photoreceptors; OS = outer segment of photoreceptors; RPE= retinal pigment epithelium; SD = standard deviation;

\* = significant at a value  $p < 0.05$